

We are IntechOpen, the world's leading publisher of Open Access books Built by scientists, for scientists

5,800

Open access books available

142,000

International authors and editors

180M

Downloads

Our authors are among the

154

Countries delivered to

TOP 1%

most cited scientists

12.2%

Contributors from top 500 universities



WEB OF SCIENCE™

Selection of our books indexed in the Book Citation Index
in Web of Science™ Core Collection (BKCI)

Interested in publishing with us?
Contact book.department@intechopen.com

Numbers displayed above are based on latest data collected.
For more information visit www.intechopen.com



Triple-Hop Hybrid FSO/mmW Based Backhaul Communication System for Wireless Networks Applications of 5G and beyond

*Mogadala Vinod Kumar, Yenneti Laxmi Lavanya,
Bharati Bidikar and Gottapu Sasibhushana Rao*

Abstract

Wireless networks applications of 5G and beyond require high throughput and high capacity. To achieve this, a macro cell is split into several small cells. When using Free Space Optics (FSO) some of the small cell base stations (BSs) which are located at the edges of a macro cell may not directly communicate with the base station of that macro cell, resulting in high outage probability (OP) and average bit error rate (ABER). Therefore, there is a need to develop a new system model to improve the OP and ABER performance. For such scenarios, triple-hop (TH) hybrid free space optics/millimeter wave (FSO/mmW) system has been proposed by considering neighboring small cell BSs as intermediate relays to forward the backhaul data. The OP and ABER of the proposed TH hybrid FSO/mmW system are derived for various channel conditions and are further verified by performing Monte-Carlo simulations. In this work, FSO link is modeled by Gamma-Gamma distribution over weak and strong turbulence channel conditions. Further the mmW link is modeled by using Nakagami-m distribution which perfectly models various fading scenarios.

Keywords: free space optics, millimeter waves, triple-hop, outage probability, average bit error rate, gamma-gamma, Nakagami-m

1. Introduction

Mobile cellular traffic has astoundingly increased during the last decade mainly due to the stunning expansion of smart wireless devices and bandwidth demanding applications (i.e., high-definition videos, gaming, social networking, etc.). The overall mobile data traffic is expected to grow up to 77 Exabyte's per month by 2022 which is about a seven-fold increase over 2017 data traffic [1]. In addition, the number of devices and connections will continue to grow exponentially. The fifth generation (5G) networks are aimed at meeting the requirements of mobile communications even beyond 2025. Current backhaul communication of cellular networks uses licensed microwave spectrum and wired copper/fiber based links. These two systems have several limitations (e.g., low data rates, security issues, and high cost of installation in urban canyons). Choosing a suitable technology in the design of the backhaul

network architecture plays a vital role in the performance of the next generation cellular networks [2]. Wireless free-space optics (FSO) and unlicensed millimeter wave (mmW) communications are being considered as the major technologies for high data rate backhaul traffic of next generation wireless networks of 5G and beyond [3]. Millimeter wave communications can achieve data rates up to 10 Gbits/s. This is because there is a large amount of bandwidth available in the mmW band (30–300 GHz), and allocating this bandwidth is an efficient approach to enhance system capacity. FSO is a line-of-sight (LOS) technology that uses light emitting diodes (LEDs) or laser to transmit information through free space medium. FSO communication has attracted significant attention due to its unlimited bandwidth, as it operates in the unlicensed Tera Hertz spectrum band [4]. However, both the FSO and mmW links are affected by different weather conditions but are complementary in nature. Therefore, hybrid system comprising of FSO/mmW communication has the advantages of both the systems and overcomes the limitations of individual systems.

In wireless networks of 5G and beyond, a given macro cell will be covered by several small cells. In such cases, some of the small cell BSs which are located at the edges of that macro cell may not be able to communicate directly with it. Hence, there is a necessity of developing a cellular system that will be based on complex interactions between small cell base stations (SBSs) and cooperation between them is necessary in order to improve the overall performance (network coverage, reduced outage probability, spectral and power efficiency) of the system. For such scenarios, triple-hop (TH) hybrid FSO/mmW system has been proposed by considering neighboring small cell BSs as intermediate relays to forward the backhaul data. This chapter mainly focuses on the performance analysis of the proposed triple-hop hybrid FSO/mmW system, which improves the reliability and coverage between SBSs and macro cell BSs over weak and strong turbulence channel conditions. This chapter is organized as follows: Section 2 introduces the proposed system model and statistical characteristics of the system is presented in Section 3. The performance analysis of the proposed system over weak and strong turbulence channel conditions is discussed in Section 4. Section 5 presents the results and discussion, and finally conclusions are presented in Section 6.

2. Proposed system and channel models

To improve the communication between a macro cell BS and small cell BS, a decode and forward (DF) relaying based triple-hop system is proposed by considering intermediate small cell BSs as relay nodes. In this, the first relay (R_1) BS will decode the received signal from the source (S) BS and then forward it to the second relay (R_2) BS. The second relay BS decodes and forwards the received signal from first relay BS to the destination (D) BS. The proposed DF relaying based triple-hop system comprising of source (S) BS, destination (D) BS, and two relay base stations (R_1 , R_2) is shown in **Figure 1**. The FSO system communicates by using intensity modulation at the transmitter and direct detection scheme (IM/DD) at the receiver [5].

2.1 Modeling of received FSO signals at different BSs

Mathematical formulation of the received signals for FSO and mmW links at R_1 , R_2 , and D base stations are presented in this section. In the case of FSO transmission, the signal received at base station R_1 from base station S is given by

$$y_{SR_1}^{FSO} = c_{SR_1} I_{SR_1} g_{SR_1} x + n_{SR_1} \quad (1)$$

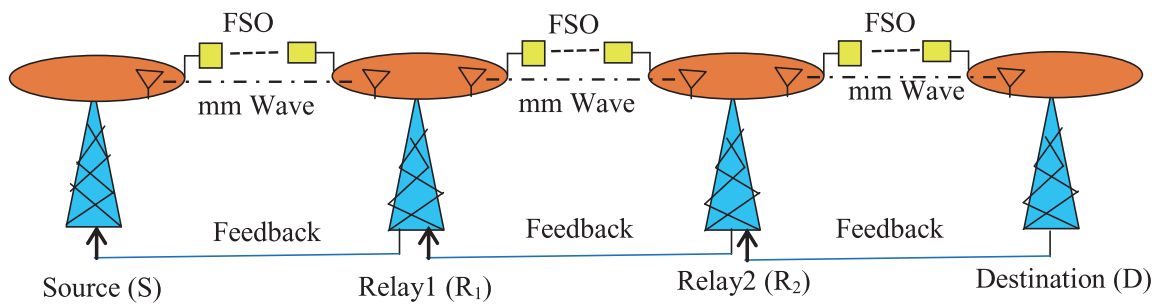


Figure 1.
Schematic of proposed triple-hop hybrid FSO/mmW system.

The signal received at base station R_1 is decoded and forwarded to base station R_2 and the signal received at base station R_2 is given by

$$y_{R_1R_2}^{FSO} = c_{R_1R_2} I_{R_1R_2} g_{R_1R_2} \tilde{x} + n_{R_1R_2} \quad (2)$$

The signal received at base station R_2 is decoded and forwarded to base station D and the signal received at base station D is given by

$$y_{R_2D}^{FSO} = c_{R_2D} I_{R_2D} g_{R_2D} \hat{x} + n_{R_2D} \quad (3)$$

where suffix SR_1 , R_1R_2 , and R_2D are source to relay1, relay1 to relay2, and relay2 to destination respectively, x is the symbol transmitted by source BS with average energy E_s , \tilde{x} is the estimate of x at R_1 , \hat{x} is the estimate of \tilde{x} at R_2 , c_j is the receiver's optical-to-electrical conversion coefficient, g_j is the average gain of the j^{th} FSO link, I_j represents the optical channel fading due to atmospheric turbulence of j^{th} link which is modeled using Gamma-Gamma distribution [6], n_j is the zero-mean circularly symmetric complex Gaussian noise of j^{th} link, where $E\{n_j n_j^*\} = \sigma_n^2$, and $j \in \{SR_1, R_1R_2, R_2D\}$. The instantaneous electrical SNR at the output of the FSO receiver denoted by γ_j^{FSO} is given as [7].

$$\gamma_j^{FSO} = \bar{\gamma}_j^{FSO} I_j^2 \quad (4)$$

where $\bar{\gamma}_j^{FSO}$ is the average SNR. By assuming perfect alignment between FSO transmitter and receiver apertures, the fading channel coefficient (I_j) probability density function (PDF) can be written as

$$f_{I_j}^{GG}(I_j) = \frac{2(\alpha\beta)^{\frac{\alpha+\beta}{2}}}{\Gamma(\alpha)\Gamma(\beta)} I_j^{\frac{\alpha+\beta}{2}-1} K_{\alpha-\beta}\left(2\sqrt{\alpha\beta I_j}\right), \quad I \geq 0 \quad (5)$$

where α and β are the small scale and large scale parameters of the scattering environment, $\Gamma(\cdot)$ is the gamma function [8], and $K_a(\cdot)$ is the modified Bessel function of the second kind of order a . The expression for the PDF of instantaneous SNR of FSO link can be obtained from Eqs. (4) and (5) as

$$f_{\gamma_j^{FSO}}^{GG}(\gamma) = \frac{\left(\frac{\alpha\beta}{\sqrt{\bar{\gamma}_j^{FSO}}}\right)^{\frac{\alpha+\beta}{2}} (\gamma)^{\frac{\alpha+\beta}{4}-1}}{\Gamma(\alpha)\Gamma(\beta)} K_{\alpha-\beta}\left(\sqrt{\frac{\alpha\beta}{\bar{\gamma}_j^{FSO}}}(\gamma)^{\frac{1}{2}}\right) \quad \text{for } \gamma \geq 0 \quad (6)$$

The above PDF expression of γ_j^{FSO} can be expressed in terms of Meijer G-function $G(\cdot)$ as [9].

$$f_{\gamma_j^{FSO}}^{GG}(\gamma) = P_1(\gamma)^{-1} G_{0,2}^{2,0} \left(\frac{\alpha\beta(\gamma)^{\frac{1}{2}}}{\sqrt{\gamma_j^{FSO}}} \middle| \begin{matrix} - \\ \alpha, \beta \end{matrix} \right) \quad (7)$$

where $P_1 = \frac{1}{2\Gamma(\alpha)\Gamma(\beta)}$. The cumulative distributive function (CDF) of instantaneous SNR of FSO link is obtained by integrating the PDF of γ_j^{FSO} and is given as

$$F_{\gamma_j^{FSO}}^{GG}(\gamma) = \int_0^\gamma f_{\gamma_j^{FSO}}^{GG}(\gamma) d\gamma = P_2 G_{1,5}^{4,1} \left(\frac{(\alpha\beta)^2 \gamma}{16\gamma_j^{FSO}} \middle| \begin{matrix} 1 \\ Q_1 \end{matrix} \right) \quad (8)$$

where $P_2 = \frac{2^{\alpha+\beta-2}}{\pi\Gamma(\alpha)\Gamma(\beta)}$ and $Q_1 = \frac{\alpha}{2}, \frac{\alpha+1}{2}, \frac{\beta}{2}, \frac{\beta+1}{2}, 0$.

2.2 Modeling of received mmW signals at different BSs

The signal received by base station R_1 from base station S, over the mmW link is given by

$$y_{SR_1}^{mmW} = h_{SR_1}x + n_{SR_1} \quad (9)$$

The decoded symbol at base station R_1 is forwarded to base station R_2 and the received signal at base station R_2 is given as

$$y_{R_1R_2}^{mmW} = h_{R_1R_2}\tilde{x} + n_{R_1R_2} \quad (10)$$

The signal received at base station R_2 is decoded and forwarded to base station D and the signal received at base station D is given by

$$y_{R_2D}^{mmW} = h_{R_2D}\hat{x} + n_{R_2D} \quad (11)$$

where h_{SR_1} , $h_{R_1R_2}$, and h_{R_2D} , are S- R_1 , R_1 - R_2 , and R_2 -D fading channel coefficients respectively. The relation between instantaneous received SNR (γ_j^{mmW}) and average SNR ($\bar{\gamma}_j^{mmW}$) of any given mmW link is given by

$$\gamma_j^{mmW} = \bar{\gamma}_j^{mmW} |h_j|^2 \quad (12)$$

where h_j is the mmW fading channel. The norm of the mmW fading channel is modeled as Nakagami-m distribution and its PDF is given by

$$f_{\gamma_j^{mmW}}(\gamma) = \left(\frac{m}{\bar{\gamma}_j^{mmW}} \right)^m \frac{(\gamma)^{m-1}}{\Gamma(m)} e^{-\frac{m\gamma}{\bar{\gamma}_j^{mmW}}} \quad (13)$$

where m indicates fading severity of the channel, $\Gamma(m)$ is the standard Gamma function, and the CDF of γ_j^{mmW} is obtained by integrating the PDF of γ_j^{mmW} and is given by

$$F_{\gamma_j^{mmW}}(\gamma) = \int_0^\gamma f_{\gamma_j^{mmW}}(\gamma) d\gamma = \frac{1}{\Gamma(m)} \gamma \left(m, \frac{\gamma m}{\bar{\gamma}_j^{mmW}} \right) \quad (14)$$

where $\gamma(a, x)$ is the lower incomplete gamma function.

3. Statistical characteristics of the proposed system model

In this section, the CDF and PDF for the proposed TH hybrid FSO/mmW system over Gamma-Gamma turbulence and Nakagami-m fading channel are derived.

3.1 Derivation of CDF and PDF of TH system over G-G atmospheric channel

The CDF of γ_{TH}^{FSO} for TH FSO transmission over G-G turbulence can be derived as

$$\begin{aligned} F_{\gamma_{TH}^{FSO}}^{GG}(\gamma) &= 1 - \prod_j \left[1 - F_{\gamma_j^{FSO}}^{GG}(\gamma) \right] \\ &= F_{\gamma_{SR_1}^{FSO}}^{GG}(\gamma) + F_{\gamma_{R_1R_2}^{FSO}}^{GG}(\gamma) + F_{\gamma_{R_2D}^{FSO}}^{GG}(\gamma) - F_{\gamma_{SR_1}^{FSO}}^{GG}(\gamma)F_{\gamma_{R_1R_2}^{FSO}}^{GG}(\gamma) \\ &\quad - F_{\gamma_{SR_1}^{FSO}}^{GG}(\gamma)F_{\gamma_{R_2D}^{FSO}}^{GG}(\gamma) - F_{\gamma_{R_1R_2}^{FSO}}^{GG}(\gamma)F_{\gamma_{R_2D}^{FSO}}^{GG}(\gamma) + F_{\gamma_{SR_1}^{FSO}}^{GG}(\gamma)F_{\gamma_{R_1R_2}^{FSO}}^{GG}(\gamma)F_{\gamma_{R_2D}^{FSO}}^{GG}(\gamma) \end{aligned} \quad (15)$$

where, $F_{\gamma_{SR_1}^{FSO}}^{GG}(\gamma)$, $F_{\gamma_{R_1R_2}^{FSO}}^{GG}(\gamma)$, $F_{\gamma_{R_2D}^{FSO}}^{GG}(\gamma)$ are CDF's of S-R₁, R₁-R₂, and R₂-D links respectively, and are given below.

$$F_{\gamma_{SR_1}^{FSO}}^{GG}(\gamma) = P_2 G_{1,5}^{4,1} \left(\frac{(\alpha\beta)^2 \gamma}{16\bar{\gamma}_{SR_1}^{FSO}} \middle| \frac{1}{Q_1} \right) \quad (16)$$

$$F_{\gamma_{R_1R_2}^{FSO}}^{GG}(\gamma) = P_2 G_{1,5}^{4,1} \left(\frac{(\alpha\beta)^2 \gamma}{16\bar{\gamma}_{R_1R_2}^{FSO}} \middle| \frac{1}{Q_1} \right) \quad (17)$$

$$F_{\gamma_{R_2D}^{FSO}}^{GG}(\gamma) = P_2 G_{1,5}^{4,1} \left(\frac{(\alpha\beta)^2 \gamma}{16\bar{\gamma}_{R_2D}^{FSO}} \middle| \frac{1}{Q_1} \right) \quad (18)$$

The PDF of γ_{TH}^{FSO} is obtained by differentiating $F_{\gamma_{TH}^{FSO}}^{GG}(\gamma)$ with respect to γ and its expression is given by

$$\begin{aligned} f_{\gamma_{TH}^{FSO}}^{GG}(\gamma) &= f_{\gamma_{SR_1}^{FSO}}^{GG}(\gamma) + f_{\gamma_{R_1R_2}^{FSO}}^{GG}(\gamma) + f_{\gamma_{R_2D}^{FSO}}^{GG}(\gamma) - f_{\gamma_{SR_1}^{FSO}}^{GG}(\gamma)f_{\gamma_{R_1R_2}^{FSO}}^{GG}(\gamma) \\ &\quad - F_{\gamma_{SR_1}^{FSO}}^{GG}(\gamma)f_{\gamma_{R_1R_2}^{FSO}}^{GG}(\gamma) - f_{\gamma_{R_1R_2}^{FSO}}^{GG}(\gamma)F_{\gamma_{R_2D}^{FSO}}^{GG}(\gamma) - F_{\gamma_{R_1R_2}^{FSO}}^{GG}(\gamma)f_{\gamma_{R_2D}^{FSO}}^{GG}(\gamma) \\ &\quad - f_{\gamma_{SR_1}^{FSO}}^{GG}(\gamma)F_{\gamma_{R_2D}^{FSO}}^{GG}(\gamma) - F_{\gamma_{SR_1}^{FSO}}^{GG}(\gamma)f_{\gamma_{R_2D}^{FSO}}^{GG}(\gamma) + f_{\gamma_{SR_1}^{FSO}}^{GG}(\gamma)F_{\gamma_{R_1R_2}^{FSO}}^{GG}(\gamma)F_{\gamma_{R_2D}^{FSO}}^{GG}(\gamma) \\ &\quad + F_{\gamma_{SR_1}^{FSO}}^{GG}(\gamma)f_{\gamma_{R_1R_2}^{FSO}}^{GG}(\gamma)F_{\gamma_{R_2D}^{FSO}}^{GG}(\gamma) + F_{\gamma_{SR_1}^{FSO}}^{GG}(\gamma)F_{\gamma_{R_1R_2}^{FSO}}^{GG}(\gamma)f_{\gamma_{R_2D}^{FSO}}^{GG}(\gamma) \end{aligned} \quad (19)$$

where $F_{\gamma_{SR_1}^{FSO}}^{GG}(\gamma)$, $F_{\gamma_{R_1R_2}^{FSO}}^{GG}(\gamma)$, $F_{\gamma_{R_2D}^{FSO}}^{GG}(\gamma)$ are given by Eqs. (16)–(18) respectively.

$f_{\gamma_{SR_1}^{FSO}}^{GG}(\gamma)$, $f_{\gamma_{R_1R_2}^{FSO}}^{GG}(\gamma)$, $f_{\gamma_{R_2D}^{FSO}}^{GG}(\gamma)$ are PDF's of S-R₁, R₁-R₂, and R₂-D links respectively, and are given below.

$$f_{\gamma_{SR_1}^{GG}}(\gamma) = P_1(\gamma)^{-1} G_{0,2}^{2,0} \left(\frac{\alpha\beta(\gamma)^{\frac{1}{2}}}{\sqrt{\gamma_{SR_1}^{FSO}}} \middle| \begin{matrix} - \\ \alpha, \beta \end{matrix} \right) \quad (20)$$

$$f_{\gamma_{R_1R_2}^{GG}}(\gamma) = P_1(\gamma)^{-1} G_{0,2}^{2,0} \left(\frac{\alpha\beta(\gamma)^{\frac{1}{2}}}{\sqrt{\gamma_{R_1R_2}^{FSO}}} \middle| \begin{matrix} - \\ \alpha, \beta \end{matrix} \right) \quad (21)$$

$$f_{\gamma_{R_1D}^{GG}}(\gamma) = P_1(\gamma)^{-1} G_{0,2}^{2,0} \left(\frac{\alpha\beta(\gamma)^{\frac{1}{2}}}{\sqrt{\gamma_{R_2D}^{FSO}}} \middle| \begin{matrix} - \\ \alpha, \beta \end{matrix} \right) \quad (22)$$

3.2 Derivation of CDF and PDF of TH system over Nakagami-m fading channel

The cumulative distribution function of γ_{TH}^{mmW} for mmW transmission is given by

$$F_{\gamma_{TH}^{mmW}}(\gamma) = 1 - \prod_j [1 - F_{\gamma_j^{mmW}}(\gamma)] \quad (23)$$

$F_{\gamma_{TH}^{mmW}}(\gamma)$ is the CDF of γ_{TH}^{mmW} over Nakagami-m fading and is obtained by using Eq. (14) as

$$F_{\gamma_{TH}^{mmW}}(\gamma) = 1 - \left[\left(\frac{\Gamma\left(m, \frac{\gamma m}{\gamma_{SR_1}^{mmW}}\right)}{\Gamma(m)} \right) \left(\frac{\Gamma\left(m, \frac{\gamma m}{\gamma_{R_1R_2}^{mmW}}\right)}{\Gamma(m)} \right) \left(\frac{\Gamma\left(m, \frac{\gamma m}{\gamma_{R_2D}^{mmW}}\right)}{\Gamma(m)} \right) \right] \quad (24)$$

where $\Gamma(a, x)$ is the upper incomplete gamma function. The PDF of γ_{TH}^{mmW} is denoted by $f_{\gamma_{TH}^{mmW}}(\gamma)$, which is obtained by differentiating $F_{\gamma_{TH}^{mmW}}(\gamma)$ with respect to γ and its expression is given by

$$f_{\gamma_{TH}^{mmW}}(\gamma) = \left(\frac{m}{\gamma_{SR_1}^{mmW}} \right)^m \frac{(\gamma)^{m-1}}{\Gamma(m)} e^{-\frac{m\gamma}{\gamma_{SR_1}^{mmW}}} + \left(\frac{m}{\gamma_{R_1R_2}^{mmW}} \right)^m \frac{(\gamma)^{m-1}}{\Gamma(m)} e^{-\frac{m\gamma}{\gamma_{R_1R_2}^{mmW}}} + \left(\frac{m}{\gamma_{R_2D}^{mmW}} \right)^m \frac{(\gamma)^{m-1}}{\Gamma(m)} e^{-\frac{m\gamma}{\gamma_{R_2D}^{mmW}}} \quad (25)$$

4. Performance analysis of the proposed TH hybrid system

The performance of the proposed TH system is evaluated by using outage probability and average BER. In this section, the expressions for outage probability and average BER of the proposed TH hybrid FSO/mmW system between source and destination BSs over Nakagami-m and Gamma-Gamma turbulence channels are derived. The outage probability expression of the proposed TH system is given by

$$P_{out}^{TH-GG} = F_{\gamma_{TH}^{FSO} GG}(\gamma_{th}^{FSO}) F_{\gamma_{TH}^{mmW}}(\gamma_{th}^{mmW}) \quad (26)$$

where $F_{\gamma_{TH}^{FSO} GG}(\gamma_{th}^{FSO})$ is obtained by replacing γ with γ_{th}^{FSO} in Eq. (15) and $F_{\gamma_{TH}^{mmW}}(\gamma_{th}^{mmW})$ is obtained by replacing γ with γ_{th}^{mmW} in Eq. (24). The transmitted data

is mapped by using BPSK modulation and then transmitted through the FSO link or the mmW link and it is assumed that both the links operate at the same data rate. The BER for BPSK modulation as a function of the instantaneous SNR is given by (Usman M., Yang H. C., and Alouini M. S., 2014)

$$p(e/\gamma) = 0.5\text{erfc}(\sqrt{\gamma}) \quad (27)$$

The average BER during non-outage period can be calculated in terms of the average BER of individual FSO and mmW links, and is given as

$$\bar{P}_b^{TH-GG} = \frac{B_{TH}^{GG}(\gamma_{th}^{FSO}) + F_{\gamma_{TH}^{FSO}}^{GG}(\gamma_{th}^{FSO})B_{TH}^{mmW}(\gamma_{th}^{mmW})}{1 - P_{out}^{TH-GG}} \quad (28)$$

where, P_{out}^{TH-GG} is given by Eq. (26) and $F_{\gamma_{TH}^{FSO}}^{GG}(\gamma_{th}^{FSO})$ is given by Eq. (15). The average BER of FSO link ($B_{TH}^{GG}(\gamma_{th}^{FSO})$) and mmW link ($B_{TH}^{mmW}(\gamma_{th}^{mmW})$) are given below. The average BER of FSO link is obtained by averaging the conditional BER of BPSK signal over the probability density function of γ_{TH}^{FSO} based on the condition $\gamma_{TH}^{FSO} > \gamma_{th}^{FSO}$ and is given as,

$$B_{TH}^{GG}(\gamma_{th}^{FSO}) = \int_{\gamma_{th}^{FSO}}^{\infty} p(e/\gamma) f_{\gamma_{TH}^{FSO}}^{GG}(\gamma) d\gamma \quad (29)$$

where $p(e/\gamma)$ and $f_{\gamma_{TH}^{FSO}}^{GG}(\gamma)$ are given by Eqs. (27) and (19) respectively. Similarly, the average BER of mmW link is obtained by averaging the conditional BER of BPSK signal over the probability density function of γ_{TH}^{mmW} based on the condition $\gamma_{TH}^{mmW} > \gamma_{th}^{mmW}$ and is given as,

$$B_{TH}^{mmW}(\gamma_{th}^{mmW}) = \int_{\gamma_{th}^{mmW}}^{\infty} p(e/\gamma) f_{\gamma_{TH}^{mmW}}(\gamma) d\gamma \quad (30)$$

where, $p(e/\gamma)$ and $f_{\gamma_{TH}^{mmW}}(\gamma)$ are given by Eqs. (27) and (25) respectively. By substituting Eqs. (29) and (30) in Eq. (28), the average BER of the TH hybrid FSO/mmW system without direct link between source and destination BSs can be obtained.

5. Results and discussion

In this section, the performance of the proposed systems are compared by evaluating the analytical expressions which are derived for outage probability and average BER over weak and strong turbulent channel conditions. The procedure followed in the implementation of the proposed TH hybrid FSO/mmW backhaul communication system over weak and strong turbulent channels is shown in **Figure 2**. The FSO link is modeled for weak and strong turbulence conditions using Gamma-Gamma distribution. The typical values of α , β for strong turbulence are 2.064, 1.342 and for weak turbulence are 2.902, 2.51 respectively. Further, mmW channel is modeled by using Nakagami-m distribution with $m = 5$.

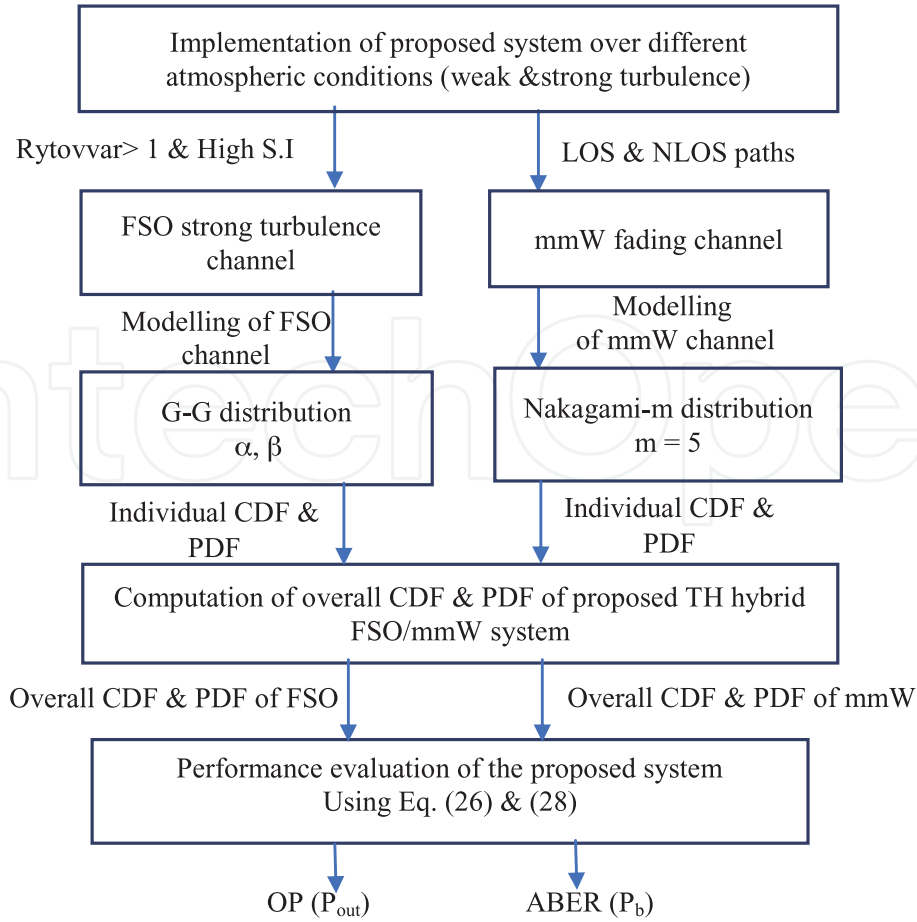


Figure 2.
Implementation of the TH hybrid FSO/mmW system over weak and strong turbulence conditions.

5.1 Outage probability vs. SNR of TH system over G-G atmospheric channel

The variation in the outage probability with respect to average SNR for FSO -TH and TH hybrid FSO/mmW systems at fixed threshold value of $\gamma_{th}^{mmW} = \gamma_{th}^{FSO} = 5 \text{ dB}$ is shown in **Figure 3**. As can be seen from **Figure 3**, the TH hybrid FSO/mmW system has better outage performance when compared to FSO-TH system, particularly when a high quality mmW link ($\gamma_{av}^{mmW} = 10 \text{ dB}$) is used. Even with a low quality mmW link ($\gamma_{av}^{mmW} = 5 \text{ dB}$), the TH hybrid system shows improvement over FSO-TH system. For instance, at 10 dB of average SNR, FSO-TH system achieves an outage probability of 8.6×10^{-1} , whereas TH hybrid FSO/mmW system achieves outage probabilities of 7.9×10^{-1} and 5.7×10^{-2} with low quality and high quality mmW links respectively. It is observed that from above results, TH hybrid system has low outage probability when compared to FSO-TH system and it is mainly due to adaptive transmission nature of TH hybrid system as it selects the transmission path based on threshold value.

The outage performance of the TH hybrid FSO/mmW system with respect to average SNR for different values of α, β with a high quality mmW link is shown in **Figure 4**. As can be seen from **Figure 4**, TH hybrid FSO/mmW system has better outage performance when compared to FSO-TH system. However, the outage performance deteriorates for strong turbulence conditions when compared to weak turbulence conditions, which is as expected. **Table 1** shows outage probability values of the FSO-TH and TH hybrid FSO/mmW system for different values of α, β with a high quality mmW link.

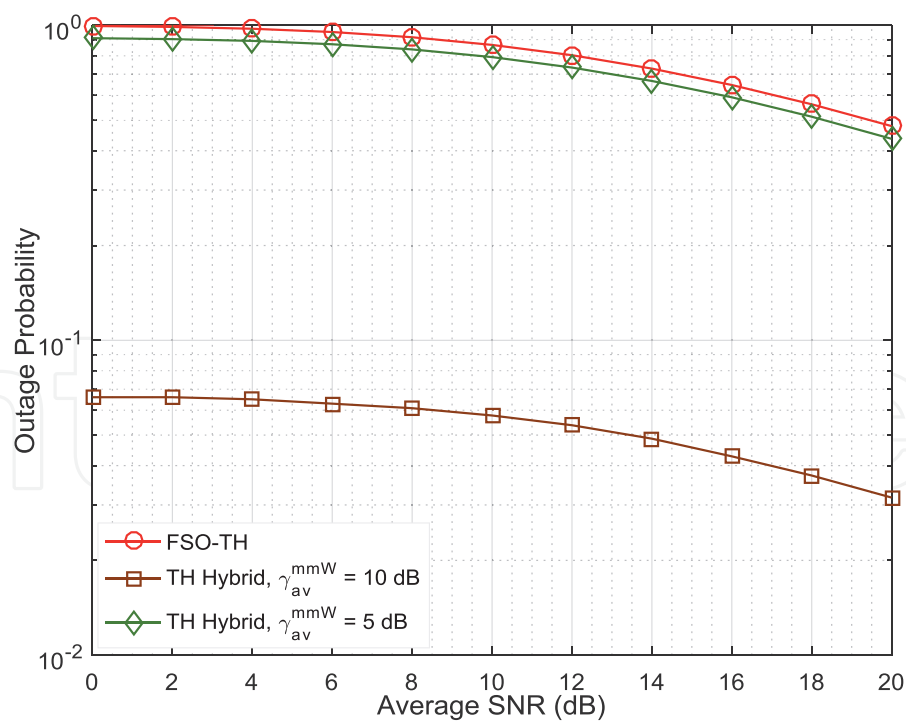


Figure 3.
Outage probability of the TH hybrid FSO/mmW system over G-G atmospheric channel.

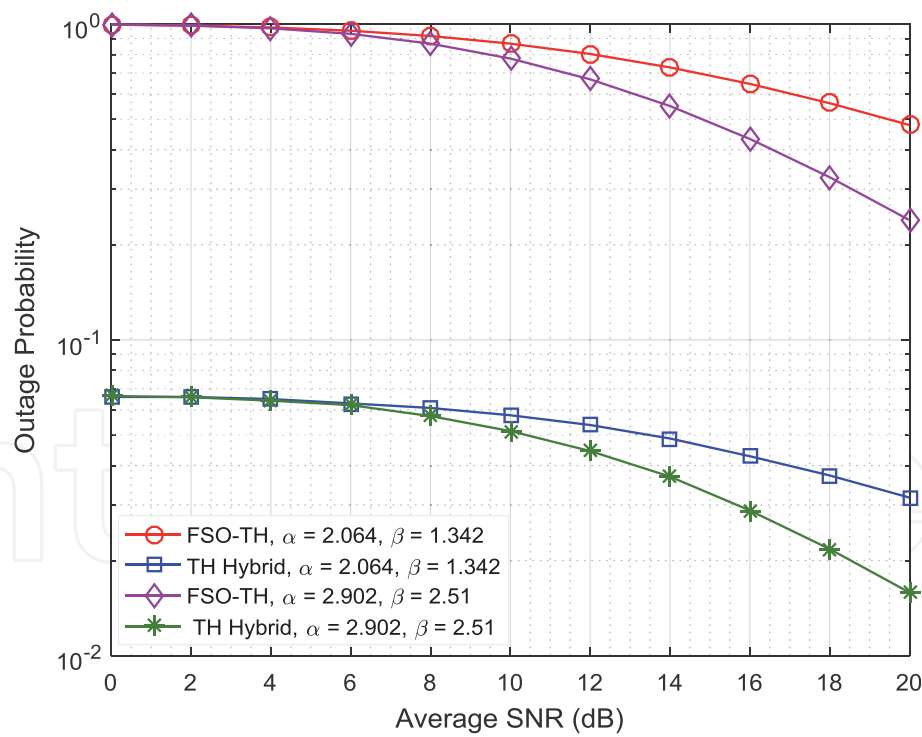


Figure 4.
Outage probability of the TH hybrid FSO/mmW system with different values of α, β over G-G atmospheric channel.

For instance, at 10 dB average SNR, the TH hybrid FSO/mmW system achieves outage probabilities of 5.1×10^{-2} and 5.7×10^{-2} , while FSO-TH system achieves outage probabilities of 7.7×10^{-1} and 8.6×10^{-1} , respectively, for weak and strong turbulence channel conditions.

S.No.	Avg. SNR (dB)	FSO-TH system		TH hybrid system	
		$\alpha = 2.902$ $\beta = 2.51$	$\alpha = 2.064$ $\beta = 1.342$	$\alpha = 2.902$ $\beta = 2.51$	$\alpha = 2.064$ $\beta = 1.342$
1	2	9.8×10^{-1}	9.8×10^{-1}	6.5×10^{-2}	6.5×10^{-2}
2	4	9.6×10^{-1}	9.7×10^{-1}	6.4×10^{-2}	6.4×10^{-2}
3	6	9.3×10^{-1}	9.5×10^{-1}	6.2×10^{-2}	6.2×10^{-2}
4	8	8.6×10^{-1}	9.1×10^{-1}	5.7×10^{-2}	6.0×10^{-2}
5	10	7.7×10^{-1}	8.6×10^{-1}	5.1×10^{-2}	5.7×10^{-2}
6	12	6.6×10^{-1}	8.0×10^{-1}	4.4×10^{-2}	5.3×10^{-2}
7	14	5.5×10^{-1}	7.2×10^{-1}	3.6×10^{-2}	4.8×10^{-2}
8	16	4.3×10^{-1}	6.4×10^{-1}	2.8×10^{-2}	4.2×10^{-2}
9	18	3.2×10^{-1}	5.6×10^{-1}	2.1×10^{-2}	3.7×10^{-2}
10	20	2.3×10^{-1}	4.7×10^{-1}	1.5×10^{-2}	3.1×10^{-2}

Table 1.
Outage probability of FSO-TH and TH hybrid FSO/mmW vs. average SNR over G-G atmospheric channel.

5.2 ABER vs. SNR of TH system over G-G atmospheric channel

The variation in the average BER of the TH hybrid FSO/mmW system with respect to the average SNR for a fixed threshold value of $\gamma_{th}^{mmW} = \gamma_{th}^{FSO} = 5dB$ is shown in **Figure 5**. As can be seen from **Figure 5**, the TH hybrid FSO/mmW system has better ABER performance when compared to FSO-TH system. With a high quality mmW link ($\gamma_{av}^{mmW} = 10dB$), there is only marginal improvement in ABER performance, especially over low SNR region. This is because at a very low value of average SNR of FSO link, the high quality mmW link is being used more frequently. As average SNR of FSO link improves, the FSO link will be used for transmission

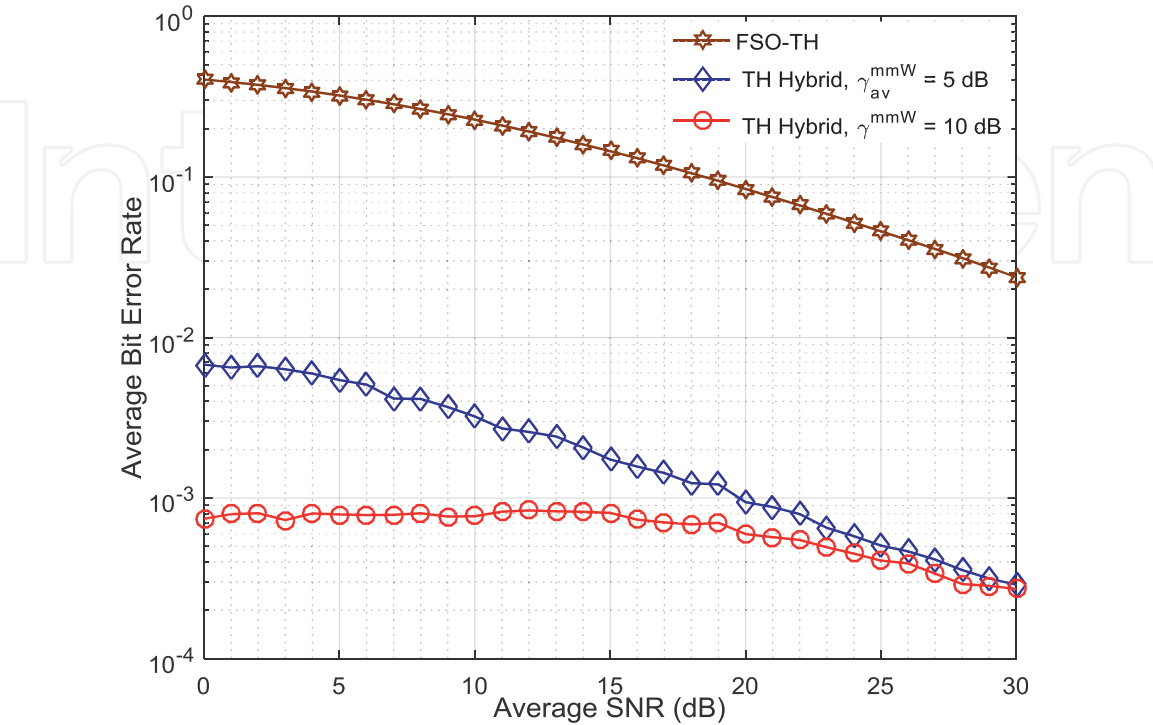


Figure 5.
ABER of the TH hybrid FSO/mmW system over G-G atmospheric channel.

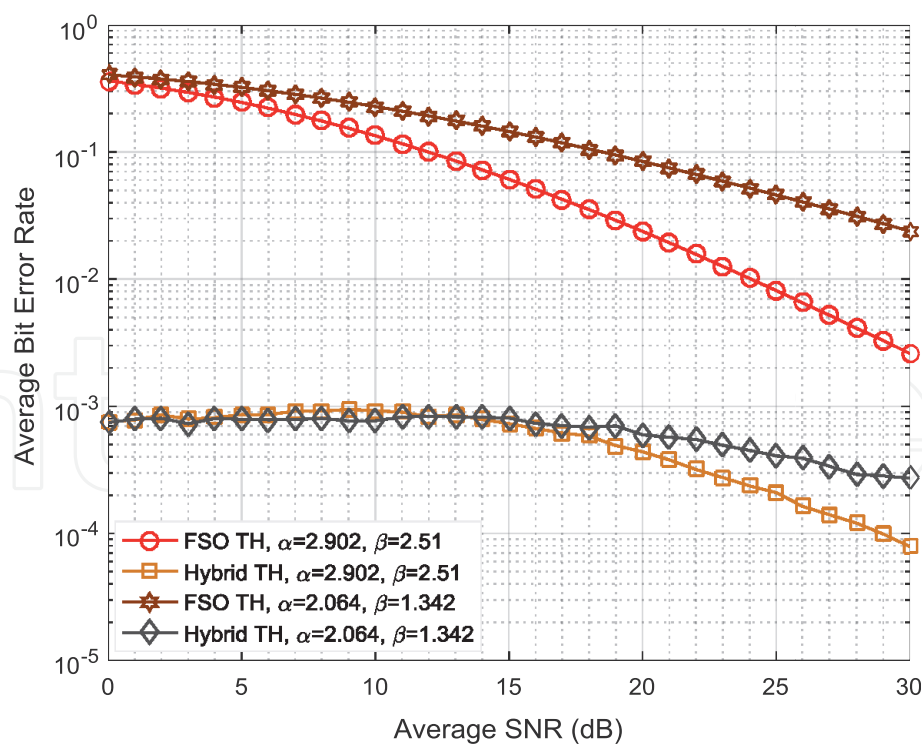


Figure 6.
ABER of the TH hybrid FSO/mmW system for different values of α , β over G-G atmospheric channel.

and hence the ABER performance of the TH hybrid FSO/mmW system improves further. For instance, at 10 dB of average SNR, FSO-TH system achieves an ABER of 2.2×10^{-1} , whereas TH hybrid FSO/mmW system achieves ABER of 3.2×10^{-3} and 7.7×10^{-4} with low quality ($\gamma_{av}^{mmW} = 5\text{dB}$) and high quality ($\gamma_{av}^{mmW} = 10\text{dB}$) mmW links respectively.

Figure 6 shows the ABER performance of the FSO-TH and TH hybrid FSO/mmW systems with respect to average SNR for different values of α and β . As can be seen from **Figure 6**, TH hybrid FSO/mmW system has better ABER performance when compared to FSO-TH system. The ABER values of FSO-TH and TH hybrid FSO/mmW systems for different values of α , β with a high quality mmW link are tabulated in **Table 2**.

S.No	Avg. SNR (dB)	FSO-TH		TH Hybrid	
		$\alpha = 2.902$ $\beta = 2.51$	$\alpha = 2.064$ $\beta = 1.342$	$\alpha = 2.902$ $\beta = 2.51$	$\alpha = 2.064$ $\beta = 1.342$
1	5	2.4×10^{-1}	3.2×10^{-1}	8.6×10^{-4}	7.9×10^{-4}
2	10	1.3×10^{-1}	2.2×10^{-1}	9.2×10^{-4}	7.7×10^{-4}
3	12	9.9×10^{-2}	1.9×10^{-1}	8.2×10^{-4}	8.3×10^{-4}
4	14	7.2×10^{-2}	1.5×10^{-1}	7.8×10^{-4}	8.2×10^{-4}
5	16	5.0×10^{-2}	1.3×10^{-1}	6.6×10^{-4}	7.3×10^{-4}
6	18	3.5×10^{-2}	1.0×10^{-1}	5.8×10^{-4}	6.8×10^{-4}
7	20	2.3×10^{-2}	8.4×10^{-2}	4.3×10^{-4}	5.9×10^{-4}
8	24	1.0×10^{-2}	5.2×10^{-2}	2.3×10^{-4}	4.5×10^{-4}
9	28	4.1×10^{-3}	3.1×10^{-2}	1.2×10^{-4}	2.9×10^{-4}
10	30	2.5×10^{-3}	2.3×10^{-2}	7.8×10^{-5}	2.7×10^{-4}

Table 2.
ABER of FSO-TH and TH hybrid FSO/mmW vs. average SNR over G-G atmospheric channel.

For instance, at 20 dB average SNR, FSO-TH system achieves ABER of 2.3×10^{-2} and 8.4×10^{-2} , while TH hybrid FSO/mmW system achieves ABER of 4.3×10^{-4} and 5.9×10^{-4} , respectively for weak and strong turbulence conditions.

6. Conclusions

Performance analysis of the proposed TH hybrid FSO/mmW system for macro-cell BS to small cell BS backhaul communication has been carried out in this chapter. The FSO link turbulence conditions ranging from weak to strong are modeled by using Gamma-Gamma distribution. Further, mmW channel is modeled by using Nakagami-m distribution with $m = 5$. Outage probability and ABER of the TH scenario have been analyzed for different values of α , β over Gamma-Gamma distribution and average SNR of mmW links. From the results, it is concluded that TH hybrid FSO/mmW system has improved outage and ABER performance when compared to FSO-TH system.

Acknowledgements

The work presented in this paper is supported by Visvesvaraya PhD scheme for Electronics and IT, Ministry of Electronics and Information Technology (Meity), Government of India, being implemented by Digital India Corporation.

Author details


Mogadala Vinod Kumar^{1*}, Yenneti Laxmi Lavanya², Bharati Bidikar² and Gottapu Sasibhushana Rao²

1 Department of Electronics and Communication Engineering, Bapatla Engineering College, Bapatla, Andhra Pradesh, India

2 Department of Electronics and Communication Engineering, Andhra University, Visakhapatnam, Andhra Pradesh, India

*Address all correspondence to: vinodkumar.mogadala@becbapatla.ac.in

IntechOpen

© 2022 The Author(s). Licensee IntechOpen. This chapter is distributed under the terms of the Creative Commons Attribution License (<http://creativecommons.org/licenses/by/3.0>), which permits unrestricted use, distribution, and reproduction in any medium, provided the original work is properly cited. 

References

- [1] Cisco. Visual Networking Index: Forecast and Trends, 2017–2022, White Paper. [Internet] 2019. Available from: <https://s3.amazonaws.com/media.media-post.com/uploads/CiscoForecast.pdf>
- [2] Mogadala VK, Gottapu SR, Chapa BP. Dual hop hybrid FSO/RF based backhaul communication system for 5G networks. In: Proceedings of the IEEE International Conference on Wireless Communications Signal Processing and Networking (WiSPNET). Chennai, India: IEEE; 2019. pp. 229-232
- [3] Sharma S, Madhukumar AS, Swaminathan R, Sheng CJ. Performance analysis of hybrid FSO/RF transmission for DF relaying system. In: Proceedings of the IEEE Globecom Workshops (GC Wkshps). Singapore: IEEE; 2017. pp. 1-6
- [4] Ghassemlooy Z, Popoola W, Rajbhandari S. Optical Wireless Communications: System and Channel Modeling with MATLAB. 1st ed. Boca Raton: CRC Press Taylor and Francis Group; 2012. p. 497
- [5] Usman M, Yang HC, Alouini MS. Practical switching-based hybrid FSO/RF transmission and its performance analysis. IEEE Photonics Journal. 2014; 6:1-13. DOI: 10.1109/JPHOT.2014.2352629
- [6] Al-Habash MA, Andrews L, C, and Phillips R. L. Mathematical model for the irradiance probability density function of a laser beam propagating through turbulent media. Optical Engineering. 2001;8. DOI: 10.1117/1.1386641
- [7] Chatzidiamantis ND, Karagiannidis GK, Kriezis EE, Matthaiou M. Diversity combining in hybrid RF/FSO systems with PSK modulation. In: Proceedings of the IEEE International Conference on Communications (ICC). Kyoto, Japan: IEEE; 2011. pp. 1-6
- [8] Gradshteyn IS, Ryzhik IM. Table of Integrals, Series, and Products. 8th ed. Elsevier Academic Press; 2014. p. 1133. DOI: 10.1016/C2010-0-64839-5
- [9] Rakia T, Yang H, Alouini M, Gebali F. Outage analysis of practical FSO/RF hybrid system with adaptive combining. IEEE Communications Letters. 2015;19:366-369. DOI: 10.1109/LCOMM.2015.2443771